Phytopathologia Mediterranea (2017), 56, 3, 379–391
DOI: 10.14601/Phytopathol_Mediterr-20252

RESEARCH PAPERS

Ultrastructural effects of PVY^{NTN} infection of *Capsicum annuum* L. cv. Yolo Wonder generative organs; a first step in describing seed transmission

Katarzyna OTULAK[1], Edmund KOZIEŁ[1], Benham E.L. LOCKHART[2] and Grażyna GARBACZEWSKA[1]

[1] Warsaw University of Life Sciences – SGGW, Faculty of Agriculture and Biology, Department of Botany, Nowoursynowska 159, 02-776 Warsaw, Poland
[2] Department of Plant Pathology, University of Minnesota, 495 Borlaug Hall, 1991 Upper Buford Circle, St. Paul, MN 55108,USA

Summary. *Potato virus Y* ^{NTN} (PVY^{NTN}), a member of the family *Potyviridae*, is one of the most important plant viruses. Despite common occurrence of seed transmission process in the *Potyviridae*, the number or routes of virion entry into seeds are still unclear. Embryos could probably be infected either through host embryogenesis processes or via infection of reproductive tissues, therefore both processes of virus transmission in seeds and pollen grains are likely to be related. Infection by PVY has been studied in detail in host vegetative organs. We investigated, for the first time the impact of infection by the necrotic strain of PVY on *Capsicum annuum* reproductive organs. We found PVY^{NTN} particles inside *C. annuum* pollen grains and on the exine surfaces, and PVY epitopes were also found in pollen tubes. We postulate that the male gametophyte in *C. annuum* could be a source of PVY infection, which may have significance in self-pollinated hosts. We also demonstrated that PVY^{NTN} particles could be detected inside *C. annuum* seeds on embryo surfaces, while particles and *Potyvirus* inclusion bodies were observed in endothelium layers. These were mainly detected inside ovarian tissues, that is, in the ovular integuments and nucelli. Changes in both gametophytes strongly indicate that generative organs were a source of PVY^{NTN} infection. Furthermore, we have demonstrated that in *C. annuum,* PVY was transmitted vertically via seeds.

Key words: immunolocalization, transmission electron microscopy, ovary, pollen transmission, plant viruses.

Introduction

Potato virus Y (PVY), the type member of the genus *Potyvirus* (family Potyviridae), occurs commonly in economically important crops around the world (Blanchard *et al*., 2008). The most important hosts for all strains of PVY are *Solanum tuberosum*, *Nicotiana tabacum*, *Solanum lycopersicum*, and *Capsicum annuum*, as well as ornamental plants (e.g. dahlia and petunia) and many wild plant species. In host vegetative organs, the most important PVY transmission mechanisms are transport by aphid vectors and direct contact between plants (Kerlan, 2006; Quenouille *et al*., 2013). Therefore, PVY is one of the five most economically damaging viruses, hosts in the *Solanaceae* and other important families such as *Chenopodiaceae* and *Fabaceae* (Cai *et al*., 2011). Symptoms induced by PVY infection include leaf mosaic and mottling, and leaf vein, stem and petiole necroses. PVY^{NTN} isolates have most of the biological characteristics of the PVY necrotic group. Despite this, they were distinguished from PVY^{N} isolates by the ability to induce necrosis on potato tubers (Potato Tuber Necrosis Ringspot Disease; PTNRD) (Beczner *et al*., 1984; Draper *et al*., 2002). It is estimated that about 20% of virus plant pathogens can be seed-transmitted, and about one-third can be transmitted in this way in at least one host (Stace-Smith and Hamilton, 1988; Johansen *et al*., 1994). *Potyvirus* seed transmission is common-

Corresponding author: K. Otulak
E-mail: katarzyna_otulak@sggw.pl

www.fupress.com/pm
Firenze University Press
ISSN (print): 0031-9465
ISSN (online): 1593-2095

place, but the number of virions entering host seeds, and the mechanisms by which the virus enters seeds are also still unknown. Moreover, Caroll (1981) demonstrated that *Barley stripe mosaic virus* invaded host embryos indirectly through infection of meristematic tissues in the early plant development.

The mechanisms of virus transmission via seed and pollen grains may be closely related (Hull, 2004; Card *et al*., 2007). Caroll (1972, 1981) and Johansen *et al*., (1994) postulated that seed transmission can occur either through contamination of seed surfaces or infection of embryos. Infection of embryos could occur either during embryogenesis processes or indirectly by infection of the generative organ tissues before embryogenesis (Card *et al.,* 2007). Levels of virus seed transmission may be the result of a combination of both routes of infection. Data on vertical transmission of virions via pollen grains have been derived mainly from histopathological studies of infected plants (Card *et al.*, 2007).

In addition to seed transmission, transmission by pollen has also been reported for a few potyviruses, but virus influence on flower development biology and mechanisms or virus movement have not been studied. There has been no evidence for presence of PVY in seeds. Our previous studies focused principally on ultrastructural changes and systemic transport as effects of PVY infection on solanaceous plants with different resistance levels (Otulak and Garbaczewska, 2010). Those results applied primarily to plant organs not associated with generative reproduction (Otulak and Garbaczewska, 2012; Otulak and Garbaczewska, 2014). However, recent research has indicated significant impacts of several potyviruses on host generative organs and/or seeds, but not for PVY (Jonhson *et al.,* 2013; Simmons *et al.,* 2013; Bashar, 2015; Novakova *et al.*, 2015). From the results obtained, it was concluded that *Capsicum annuum* plants also react with decreased numbers of developed flowers and fruits in comparison to healthy plants. Based on these results, the present study was a "first look" at generative organ alterations and potential PVY^{NTN} infections in ovaries with ovules and pollen. The objective was to determine whether PVY could be detected in host male and female gametophytes and subsequently seeds.

Material and methods

Plant and virus

Capsicum annuum cv. Yolo Wonder plants (susceptible to PVY isolates, Arroyo *et al.,* 1996; Palloix *et al.,* 2009) were grown at 18°C, under 16 h/8 h light/dark photoperiod and at light intensity of 400 μmol m^{-2} s^{-1}. Test plants were inoculated mechanically as described previously (Otulak *et al.* 2016) at the four leaf growth stage with the NTN strain of PVY (PVY^{NTN}; provided from IHAR-PIB, Plant Breeding and Acclimatization Institute, Młochów Research Center). Flower stamens, ovaries, and seeds were collected regularly from infected and healthy plants. Fragments of vegetative organs from the next generation plants (developed from infected seeds) – especially leaves and petioles, were also collected. As mentioned in Otulak *et al*. (2016), the research was conducted into early developmental stage ("flower bud", approx. 50 d after PVY^{NTN} inoculation) and at full flower development ("mature flower", 60 d after PVY^{NTN} inoculation). Control plants were treated only with phosphate buffer. Inoculated plants were tested by DAS-ELISA (Chrzanowska & Doroszewska, 1997) for PVY infection.

Analysis of host ultrastructure using transmission electron microscopy (TEM)

Stamens, ovaries, seeds, and leaves (from next generation tested plants) were fixed as described by Karnovsky (1965), then in 2% (w/v) osmium tetroxide solution in 0.05M cacodylate buffer for 2 h at 4°C (Fink, 1960; Otulak *et al.,* 2016). Samples were dehydrated in ethanol series and embedded in Epoxy resin (Epon812, Sigma), with polymerization for 24 h at 60°C (Fink, 1960). Semi-thin sections (2–5 μm) were collected on glass slides for histological staining using crystal violet, examined using an Olympus AX 70 Provis microscope with light and fluorescent modes, and photographed using an Olympus SC35 camera. Sections (70–80 nm) were obtained using a UCT ultramicrotome (Leica Microsystems) and collected on formvar-coated copper grids. Grids were stained with 1.2% uranyl acetate and 2.5% lead citrate, and then were examined using a 268D Morgagni TEM (FEI) at 80 kV. Images were captured with a Morada digital camera (Olympus SIS).

Immunolocalization of the PVY^{NTN} epitope

Localization of PVY^{NTN} in infected *capsicum* tissues was performed following the method presented by van Lent and Verduin (1986); using primary mouse antibodies specific for PVY^{NTN} (Bioreba AG).

Immunofluorescence analysis

Fragments of host anthers and ovaries were fixed in 4% (w/v) paraformaldehyde (PFA) in 0.1 M microtubule stabilizing buffer (MSB; pH 6.9) with 0.1% (v/v) Triton X-100 for 2 h at room temperature, as described in Gubler (1989). Samples were dehydrated in ethanol with 10 mM dithiothreitol (DTT) and infiltrated in a mixture of butyl-methyl-methacrylate (BMM) resin with ethanol in dilutions of 1:3, 1:1, 3:1, and finally pure BMM. Polymerization was done by UV irradiation for 20 h at -20°C. Acetone was used to remove the BMM from 2.5 μm thick sections collected on silane slides (Thermo-Fischer Scientific). Immunofluorescence analysis was carried out after pre-incubation in 3% (w/v) BSA in phosphate-buffered saline (PBS) for 1 h at room temperature. Material was incubated with PVY^{NTN} mouse antibodies in PBS buffer in dilution 1:50 for 2 h in a humid chamber. Controls were prepared with mock-inoculated material, pre-immune serum in incubation medium or when primary antibody was omitted. Slides washed with PBS-Tween20 buffer were treated at room temperature (RT) in the dark for 2 h with secondary goat anti-mouse IgG conjugated to fluorescein isothiocyanate (FITC; Ex 495/Em 520; Sigma-Aldrich) in PBS buffer. Sections were treated with PBS and stained with 4',6-diamidino-2-phenylindole (DAPI; Invitrogen Inc.) solution (1 μg mL^{-1}, Ex 358/Em 461) for 5 min. An Olympus AX70 Provis microscope with a UM61002 filter set and equipped with an Olympus SC35 camera was used for fluorescence imaging.

Immunogold labelling of ultrathin sections and labelling quantification

Formvar-coated nickel grids with 50–70 nm-thick sections were treated with 10% hydrogen peroxide solution for 10 min to remove the resin. The grids were pre-incubated for 1 h in blocking medium containing 2% normal goat serum (Thermo-Fischer Scientific) with 3% BSA in 0.1 M PBS buffer (pH 7.6), as described previously by Otulak and Garbaczewska (2012). The grids were then rinsed three times in PBS buffer with 0.05% Tween-20 for 10 min, and then treated for 2 h at room temperature with primary mouse PVY^{NTN} antibodies (1:50) in PBS buffer. Samples were washed in PBS-Tween20 buffer. The slots were then treated for 1 h with gold-conjugated secondary anti-mouse antibody (15 nm, Sigma-Aldrich) and were then treated firstly in buffer and secondly in distilled water for 5 min. Labelling specificity was checked by incubating grids with material from mock-inoculated plant tissues, or by the primary antibody omitted from incubating solution. The grids were counterstained with 1% uranyl acetate for 5 min. and washed with distilled water for 5 × 2 min. Immunogold-labelled sections on grids were observed by electron microscope (as described above).

Immunogold labelling results in generative host organs were further analyzed. Quantification assessment of preferential labelling of specific tissues, cells or structures/organelles was carried out. Reliable estimation of gold labelling relative labelling index (RLI) was determined as described by Mayhew (2011). The direct estimation method of RLI was selected by comparison of the observed gold particles (G_0) values of selected compartments with the expected gold particles (G_e) of the appropriate reference structure (cell, tissue, or region) in generative organs (Mayhew, 2011). For estimation of G_0 and G_e, gold particles were scored in 35 9 μm^2 fields per photo. When there is random labelling, RLI=1, but where there is preferential labelling, RLI > 1. Statistical significance of preferential labelling was assessed by partial X^2 analysis (Mayhew, 2011). Statistically significant RLI values were >1, and where the corresponding partial X^2 value accounted for a substantial proportion (at least 10%) of total X^2 (Mayhew, 2011).

Double antibody sandwich ELISA (DAS-ELISA)

DAS-ELISA was performed following the protocols previously described by Chrzanowska and Doroszewska (1997). Three groups of plants were tested for the presence and titre of PVY^{NTN}. In each group 15 plants were selected. The first consisted of *C. annuum* plants with PVY symptoms from which seeds have been obtained (mother plants). The second consisted of next generation *C. annuum* (germinated from collected seeds) in which we observed PVY inclusions or particles. The final group consisted of mock-inoculated *C. annuum* plants (negative control, NC). From all groups samples of leaf blades was collected. The test was done using monoclonal antibodies against PVY^N and DAS-ELISA reagents (BIOREBA AG) and a positive PVY^{NTN} control provided by BIOREBA AG. Absorbance was measured at 405 nm and a sample was considered positive, if the absorbance was at least three times greater than that of negative control (Khan *et al.*, 2003).

Statistical analyses

Statistical analyses of data obtained during the 3 year study were carried out as previously described by Otulak *et al.* (2016) with one modification, namely assessment of *C. annuum* plants germinated from collected seeds. Analyses were carried out using the software STATISTICA with the one-factor analysis of variance (ANOVA) method. The statistical significance of variances and means of fruit, flowers, and seeds between healthy and PVY^{NTN}-infected plants were appraised with *P*-values < 0.05, determined by Tukey's HSD test. In 2014, 2015 and 2016 we assessed the generative organs of 45 mock-inoculated plants (15 plants per year) and 45 PVY infected *C. annuum* plants (15 plants per year). In each year, seed transmission was assessed on a group of randomly selected seeds (approx. 90 per year). Seedlings from seeds were cultivated to the four leaf stage. Next, fragments of leaf blades were fixed and embedded according to the procedure described above. Presence or absence of PVY^{NTN} in generative organs and seeds was determined on the basis of TEM observation of ultrathin sections from PVY^{NTN}-inoculated *C. annuum* plants.

Results

Flower buds and mature flowers of *Capsicum* plants infected with PVY^{NTN} were incrementally collected over the experimental period and used for histological and ultrastructural investigations. Starting from 15 d after PVY^{NTN} inoculation, leaf mosaic and dark green vein banding on leaf blades were observed on infected *C. annuum* plants. Approximately 2 months post-inoculation, the plants developed typical chlorotic symptoms on leaf blades and fruit deformation. Petiole fall and partial defoliation were also noticed. After inoculation the plants developed fewer flowers and fruits in comparison to mock-inoculated controls. Some plants showed inhibited fruit development, as well as reductions in seeds formation. PVY infection of causes observable changes in quantity of flowers and, in the long term, also fruits. PVY^{NTN}-infected plants had approx. 38.6% fewer flowers, as well as fruits, compared to mock-inoculated controls. Parallel analysis indicated that plants inoculated/infected by PVY^{NTN} had fewer seeds than mock-inoculated controls. In inoculated plants, 28% fewer seeds were formed. Furthermore, in 30% of seeds in infected plants, PVY^{NTN} virions were detected. Therefore, this report is focused on ultrastructural studies of changes/malformations in host organs crucial for generative reproduction during PVY^{NTN} infection. Macroscopic dissection of *C. annuum* ovaries did not reveal any structural modifications, but histological analysis revealed necrotisation in the placental area, despite normal ovule formation. Mock inoculated plants did not have altered anthers and/or ovaries.

Alterations of *C. annuum* generative elements resulting from PVY^{NTN} infection

Analysis of infected ovaries and ovules and virus immunolocalization

Examination of ovary tissues by TEM revealed the presence of PVY^{NTN} virions in the parenchymas of *C. annuum* plants. Necrotic changes observed within the placental areas occurred most frequently in vascular bundles, that is, in phloem tissue, where *potyvirus*-induced cytoplasmic inclusions were extensively visible in necrotic and collapsed companion cells (Figure 1a). PVY^{NTN} particles or cytoplasmic inclusions were not observed in ovary xylem elements. PVY^{NTN} virions were also observed in ovary walls and in parenchyma cells of placentae, usually inside vacuoles in the vicinity of electron-dense granules with vesicles (Figure 1b).

Ultrastructural investigation of the ovules indicated that PVY^{NTN} particles were located only within parenchyma tissues of the ovule sheaths, particularly in the region of necrotized cytoplasm of parenchyma cells (Figure 1c). In a significant number of ovules, PVY^{NTN} occurred as particle clusters in the nucellus cell cytoplasm (Figure 1d). No viral particles were observed in mature embryo sacs.

The epitope of PVY^{NTN} (green fluorescence signal) was detected in the vascular bundles as well as parenchyma cells of ovary walls (Figure 1e). Strong fluorescence signals, that is PVY^{NTN} localization, were observed in parenchyma cells and around vascular tissues of ovarian placentae during flower maturation (between 50 to 60 d after viral inoculation), and also inside ovules (Figure 1f). The fluorescence signal in ovules was more intense 2 months after the PVY^{NTN} inoculation in comparison to analyses of control ovary tissue (Figure 1g). Immunogold labelling revealed localization of gold granules, associated with PVY^{NTN} particles. This was affirmed by localization of the PVY^{NTN} epitope inside xylem vas-

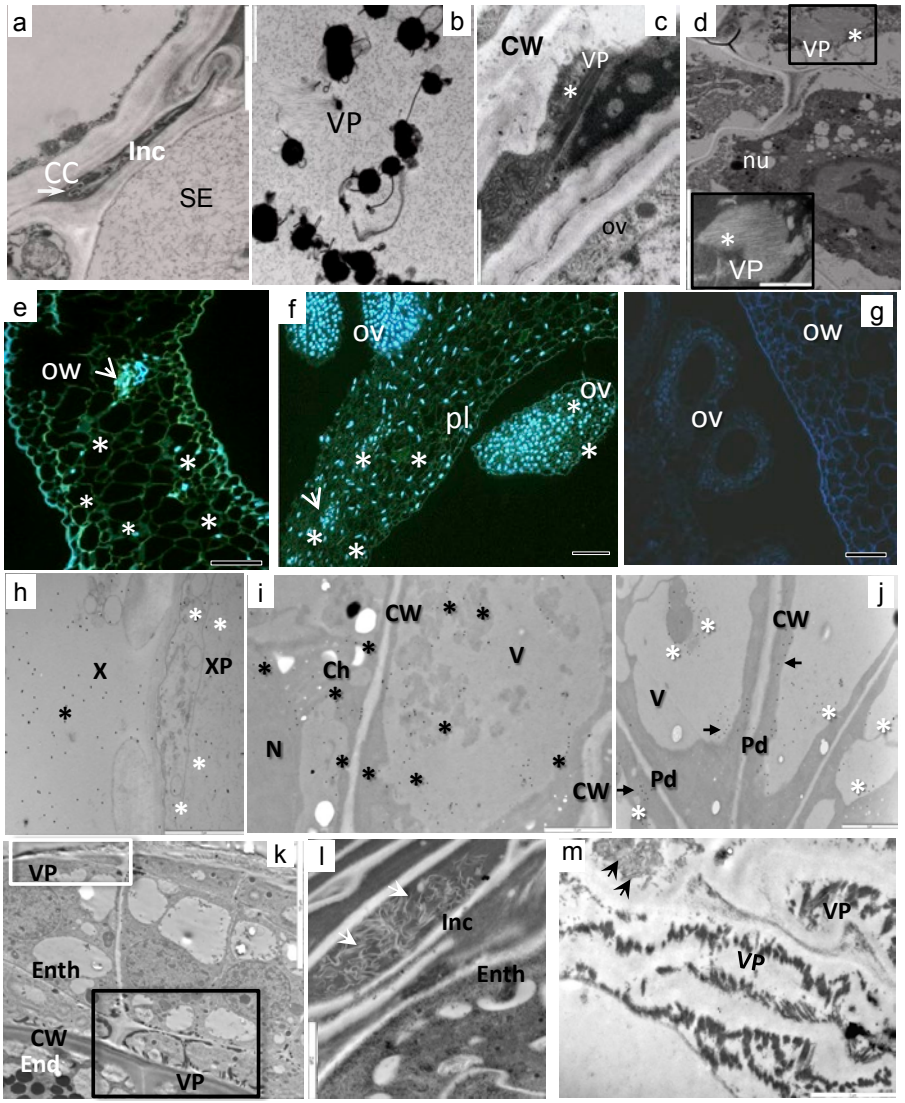

Figure 1. Ultrastructural analysis (a-d) with PVY ^{NTN} immunolocalization (e-j) of infected *Capsicum annuum* ovary (a-j) and analysis of *C. annuum* seeds (k-m). a) PVY ^{NTN} cytoplasmic inclusions (Inc, arrow) in necrotic and collapsed phloem cells. Bar = 2 μm. b) PVY^{NTN} particles (VP, asterisk) near electron-dense granules in a vacuole (V) of a parenchyma cell in an ovary wall. Bar = 2 μm. c) PVY particles (VP, asterisk) in necrotized areas of ovule (ov) sheath parenchyma cells. Bar = 2 μm. d) Regular inclusion of PVY particles (VP, asterisk) in nucellus cells (nu). Bar = 5 μm. In the corner, enlarged virus particles clusters. Bar = 1 μm. e) Epitope of PVY^{NTN} (green fluorescence) was located inside parenchyma cells (asterisk) and in the regions of the phloem and xylem (vascular tissues) (arrow) of ovary walls (ow). Bar = 200 μm. f) Virus localization in parenchyma cells (asterisk) and around vascular bundles (arrow) of ovarian placentae (pl). Bar = 200 μm. g) Lack of green fluorescence signal in mock-inoculated *C. annuum* ovary. Ov, ovules; ow, ovary wall. Bar = 200 μm. h) Gold granule deposition linked with the presence of PVY^{NTN} in xylem parenchyma (XP, white asterisk) and tracheary element (X, black asterisk). Bar = 2 μm. i) Colloidal gold deposition (asterisk) in a cytoplasm ovarian cell wall and inside a vacuole (V) in the vicinity of electron-dense granules. Bar = 2 μm. j) Gold granules around plasmodesmata (Pd) (arrows) and inside vacuoles (V, asterisk) in an ovule nucellus parenchyma cell. Bar = 2 μm. Ch, chloroplast; CW, cell wall. k) Flattened layer of endothelial cells (Enth) with virus particle (VP) deposition (white and black frame). Virus particles attached to the cell wall (CW). End, endosperm. Bar = 10 μm. l) Virus cytoplasmic inclusion (Inc, arrow) in the degraded layer of endothelium. Bar = 2 μm. m) Virus cytoplasmic inclusions (Inc, arrows) in electron-dense cytoplasm of collapsed layers between endosperm and embryo cells. Bar = 2 μm.

cular elements and xylem parenchyma (Figure 1h). However, the colloidal gold deposits were observed in cytoplasm of ovary cell walls and also in vacuoles in the vicinity of electron-dense granules (Figure 1i). Gold deposition was found in ovules in areas not only around plasmodesmata, but also inside vacuoles in ovule sheath parenchymal cells and/or nucellus parenchymal cells (Figure 1j). Lack of gold deposition was noted in ovaries as well as ovules from mock-inoculated plants. Analyses of RLI values and % of total X^2 confirmed preferential labelling of the PVY^{NTN} epitope in xylem parenchyma with trachea elements of ovary walls (Table 1A), as well as in ovules (Table 1C). Analyses of X^2 did not confirm PVY localization in ovaries or ovules of mock-inoculated plants (Tables 1B and 1D). Significant labelling was observed in the xylem elements inside tracheary elements (Table 1A), whereas in xylem parenchyma mainly in vacuoles (Table 1A). Preferential labelling was also associated with cytoplasm and vacuoles in other parenchyma cells (ovary walls and placentae) (Table 1A). In ovules, the viral epitope was significantly localized to vacuoles (Table 1C).

Analysis of infected seeds and PVY^{NTN} immunolocalization

Some *Capsicum* plants produced fruits with inhibited development and seeds with deformations or with visible necrotization. Ultrastructural dissection of all seeds derived from inoculated plants revealed PVY^{NTN} particle inclusions in cytoplasm, around and attached to the integument parenchymal cell walls (Figure 1k). Further observations validated previous histological examination, confirmings that PVY^{NTN} virions were deposited in the layers of endothelial cells (Figure 1k). These particles were mainly located near the cell wall areas between integument parenchymal cells and the endothelial layers, whereas the *potyvirus* cytoplasmic inclusion bodies were mainly detected in the degraded endothelium (Figures 1l-1m).

Deposition of PVY^{NTN} particles was also associated with the cell walls on the surfaces of the embryos in seeds (Figure 2a). Virus cytoplasmic inclusions were found in collapsed cells layers between embryos and endosperms (Figure 1m). PVY^{NTN} particles or inclusion depositions have not previously been observed in endosperm cell layers. Immunofluorescence localization of the PVY^{NTN} epitope was also detected for the first time in the external area of the embryos, degraded endothelial layers and in parenchyma cells of the seed coats (Figure 2a). Lack of fluorescence signal was noted in seeds from mock-inoculated *C. annuum* plants.

Effects of PVY^{NTN} infection on C. annuum *anthers, and virus immunolocalization*

The absence of PVY^{NTN} particles was observed at early stages of host plant development (buds) of stamens. Tapetum cells can degenerate before mitotic division. Further re-arrangements of neighbouring cells were observed. PVY^{NTN} virions were not observed inside endothecium cells in the early stages of differentiation. Examination of mock-inoculated plants did not reveal PVY^{NTN} particles, regardless of developmental stages of the host plant anthers. Observations of mature anthers (2 months after PVY^{NTN} inoculation) revealed tapetum cell decay, whereas pollen grains had already generative and vegetative cells (double cell stage). Invaginations were mainly observed in endothecium cell walls. Two months after the inoculation, the PVY^{NTN} cytoplasmic inclusions and virions were located in mature host stamens in tapetum remnants (Figures 2b, 2d), and in differentiated endothecium cells (Figure 2c). The PVY^{NTN} cytoplasmic inclusions were often found in necrotized vascular bundle areas. PVY^{NTN} particles in host anthers were also observed in cytoplasm of fully developed pollen grains in nuclei (Figure 2e). The PVY^{NTN} virions in mature stamens were observed on external pollen surfaces connected with exine layers. While the PVY^{NTN} cytoplasmic inclusions in anthers were usually localized in protoplasts of deformed, improperly developed pollen grains, the cytoplasmic inclusions and/or PVY^{NTN} particles were not observed in anthers and pollen grains of healthy plants.

Immunofluorescence localization of the PVY^{NTN} epitope was mainly detected in remnants of the immature tapetae and in fully developed anthers (Figure 2f). Green fluorescence exhibited inside the pollen grains and in the developing pollen tubes (Figures 2f-2g). The PVY^{NTN} signal was weak in the epidermal layers and strong in the anther walls, in parenchyma cells. Colloidal granules in pollen were localized inside pollen cytoplasm (Figure 2h), as well as on the exine surfaces, where masses of PVY^{NTN} particles were located (Figure 2h). The epitope of PVY^{NTN} was detected in the anther chambers, especially in remnants of tapetum tissue inside electron-dense masses (Figure 2i). These patterns of deposition were also seen in immature endothecium with collapsed cell layers (Figure 2i). Analyses of RLI

Table 1. Quantification of immunogold labelling by RLI and X^2 test. Assessment of immunogold labelling in PVY^{NTN} infected *C. annuum*: vascular tissue of ovary (A), ovules (C), pollen (E), anther (G) and next generation plants (H). Assessment of immunogold labelling in mock-inoculated *C. annuum* elements: ovary (B), ovule (D), pollen and anther (F). Significant values (RLI > 1, and % X^2 at least 10%) in bold font and marked with asterisk.

Sample	Parameters of immunogold labelling				
	Go	Ge	RLI	X^2 value	X^2 as %
(A) Ovary of PVY^{NTN} inoculated *C. annuum*					
- xylem vascular elements:					
cell wall	4	13.77	0.29	6.9	70
cell interior	58	48.22	**1.2***	1.98	**22.00***
Column total	62	62		8.88	100
- xylem parenchyma:					
cell wall	2	5.47	0.37	2.2	15.00
vacuole	20	13.63	**1.47***	2.98	**20.31***
cytoplasm	8	10.9	0.73	9.49	64.69
Column total	30	30		14.67	100
- Structures or compartments of ovary parenchyma cells:					
cytoplasm	68	46.67	**1.46***	9.75	**15***
vacuoles	69	46.67	**1.48***	10.68	**17***
cell wall	2	46.67	0.043	42.75	68
Column total	140	140.01		63.18	100
(B) Ovary of mock-inoculated *C. annuum*	0	0	0	0	0
(C) Ovules of PVY ^{NTN} inoculated *C. annuum*:					
- Structures or compartments:					
cytoplasm	35	59.54	0.59	76.69	77.25
vacuoles	51	26.46	**1.92***	1.49	**22.75***
Column total	86	86		78.18	100
(D) Ovule of mock-inoculated *C. annuum*	0	0	0	0	0
(E) Pollen of PVY ^{NTN} inoculated *C. annuum*:					
- External of pollen grains in context of anther chamber:					
intine	2	8.28	0.24	4.76	24.5
exine	10	4.6	**2.17***	6.34	**32.7***
anther chamber	1	3.68	0.27	1.95	10.1
viral particles	10	4.6	**2.17***	6.34	**32.7***
Column total	23	23		19.39	100

(Continued)

Table 2. (Continued).

Sample	Parameters of immunogold labelling				
	Go	**Ge**	**RLI**	**X^2 value**	**X^2 as %**
Internal of pollen grains:					
cytoplasm	34	12.4	**2.75***	37.63	**80.01***
ER	28	49.6	0.59	9.4	19.99
Column total	62	62		47.03	100
(F) Pollen and anther of mock-inoculated *C. annuum*	0	0	0	0	0
(G) Anther of PVY ^{NTN} inoculated *C. annuum*:					
anther chamber	8	37.44	0.21	23.15	51.84
tapetum	31	18.72	**1.66***	8.06	**18.03***
endothecium	39	21.84	**1.79***	13.48	**30.16***
Column total	78	78		44.69	100
(H) Leaf of next generation of *C. annuum* plants:					
- sieve tubes:					
cell interior	28	12.8	**2.19***	18.05	**58.55***
cell wall	4	19.2	0.21	12.03	41.45
Column total	32	32		30.83	100
- companion cells:	**Go**	**Ge**	**RLI**	**X^2 value**	**X^2 as %**
cell cytoplasm	38	16	**2.38***	30.25	**59.5***
cell wall	2	24	0.08	20.17	40.5
Column total	40	40		50.42	100

values and % of total X^2 confirmed preferential labelling of viral epitope in pollen cytoplasm and exine tissues and with viral particles on exine surfaces (Table 1E). Values of X^2 did not confirm presence of the PVY epitope in pollen and anthers of mock-inoculated plants (Table 1F). Significant localization was also confirmed in anthers endothecium and tapetum tissues (Table 1G). Analyzed tissues of generative organs from mock-inoculated plants and control material did not reveal green fluorescence or gold granule location, independent of the stage of infection.

The PVY^{NTN} seed transmission to the next generation of C. annuum *plants*

Three years of results of statistical analyses indicated that 66% of *C. annuum* seeds (each year about 60 seeds from 90 collected) from infected PVY^{NTN} plants germinated and formed seedlings. Further examinations indicated that approx. 30% plants from the respective next generations were infected by PVY^{NTN} (each year an average of 18 plants from 60 germinated), revealing infection symptoms. The absorbance mean values in ELISA were similar in mother (OD_{405nm} = 1,600) and next generation (OD_{405nm} = 1,500) *C. annuum* plants and also positive controls (OD_{405nm} = 1,608). In the case of positive controls, the titre values for mother and next generation plants were at least three times greater than for of the negative controls (OD_{405nm} = 0,113). Therefore, the DAS-ELISA result for presented samples was considered as positive. Presence of PVY^{NTN} in next generation plants with symptoms of viral infection

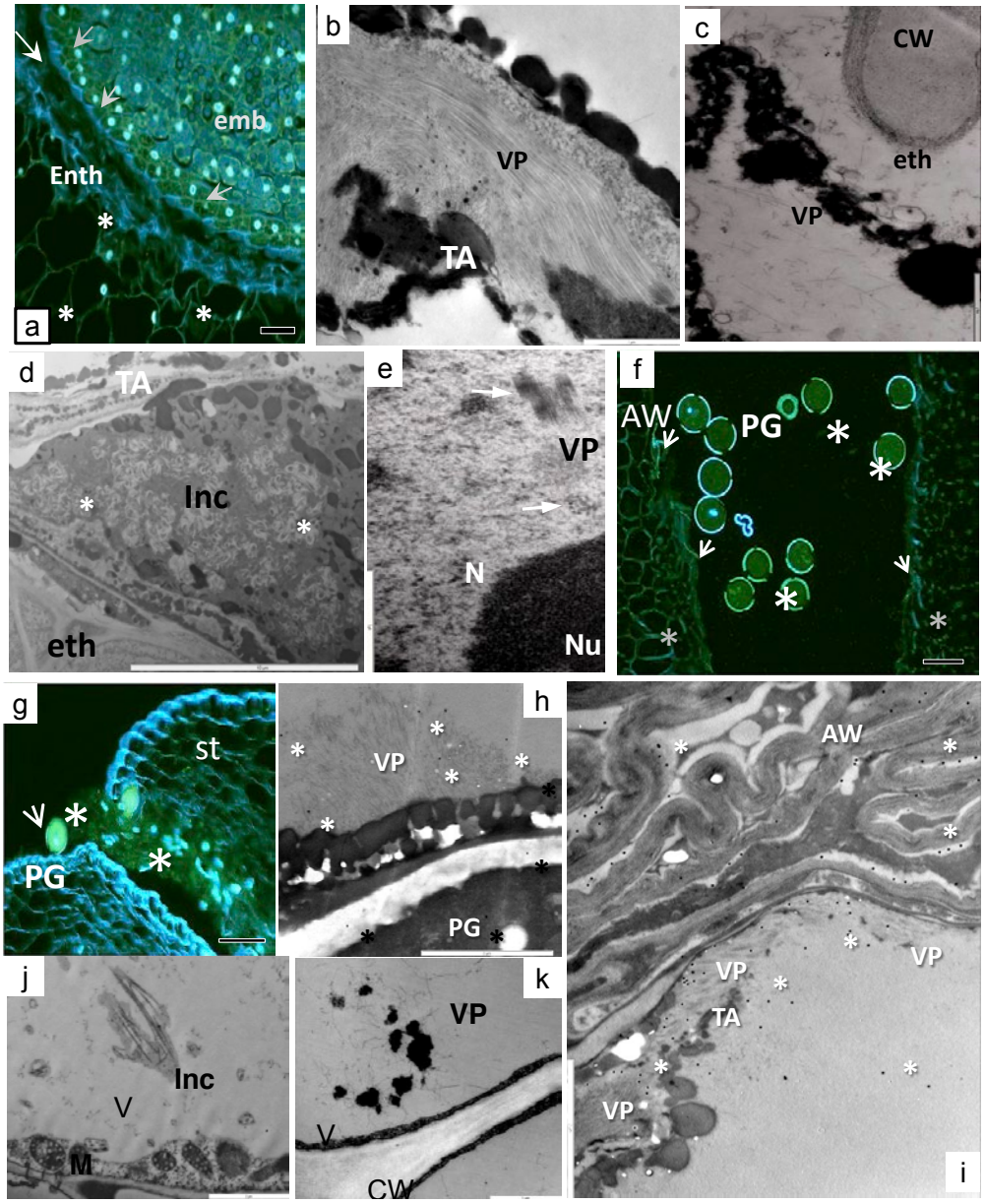

Figure 2. Examination of *C. annuum* seed embryos (a), anthers with pollen grains, (b-i) and next generation vegetative tissues (j-k). Immunolocalization of PVY^{NTN} in *C. annuum* seeds (a) and anthers (f-i). a) Green fluorescence of PVY^{NTN} epitope in degraded endothelium cell (white arrow, Enth), seed coat parenchyma cells (asterisk) and embryo (black arrow). Bar = 200 μm. b) Virus particles (VP) in rest of tapetum (TA) masses. Bar = 1 μm. c) Virus particles (VP) in differentiated a endothecium cell (eth). Bar = 1 μm. CW, cell wall. d) Virus inclusions (asterisks, Inc, pinwheels) in tapetum (TA) area. Eth, endothecium. Bar = 10 μm. e) PVY^{NTN} virions (VP, arrows) in the nucleus of a pollen grain. Bar = 1 μm. f) Green fluorescence signal in a pollen grain (white asterisk, PG), rest of tapetum (arrows) masses and in parenchyma cell of anther wall (grey asterisk, AW). Bar = 200 μm. g) Green fluorescence signal in a pollen grain (arrow) and in forming a pollen tube (asterisk). Bar = 200 μm. h) Colloidal gold deposits in virus particles (VP) on the surface (white asterisk) and inside (black asterisk) of a *C. annuum* pollen grain (PG). Bar = 2 μm. i) Colloidal gold deposits (asterisk) were observed in chambers of anthers, in remnants of tapetum cells (TA) between masses with osmophilic nature, as well as in immature endothecium cells with collapsed cells. Bar =2 μm. j) Virus inclusions (Inc) in a vacuole (V) of a mesophyll cell. Bar = 2 μm. k) PVY^{NTN} particles (VP) inside a vacuole (V) of a phloem cell. Bar =2 μm. CC, companion cell; CW, cell wall; M, mitochondria.

was also confirmed by results of DAS-ELISA tests, so PVY transfer from seeds to next generation *Capsicum* plants is postulated. Immunofluorescence detection of PVY^{NTN} in *C. annuum* leaf tissues from next generation plants indicated green fluorescence signals mainly in epidermis and vascular tissues (especially phloem, data not presented). PVY^{NTN} was also mainly detected in sieve elements and companion cells, using immunogold labelling. This was also confirmed by immunogold quantification (Table 1H). PVY^{NTN} particles (Figure 2k) and cytoplasmic inclusions (Figure 2j) were observed in mesophyll and phloem tissues, confirming systemic infection of the next generation *C. annuum* plants.

Discussion

Many viruses in plants are translocated to seeds, so virion transmission by seed is an effective mechanism of direct transfer to crop hosts. Seed transmission is therefore likely to be very significant in virus disease epidemiology, and economically in important food crops. Moreover, virions can be retained within the seeds for long periods, so propagation and dissemination of seed-borne viruses can be across long geographical ranges. Little is known regarding the specific mechanisms by which some viruses are translocated through host seeds (Hull, 2002). Seed transmission may be achieved either by invasion of embryos through ovules, or by indirect intrusion into embryos, by infected gametes. For different virus groups, both processes can take place at the same time, although the relative contribution of each may depend on a variety of factors (Wang and Maule, 1994). Johansen *et al.* (1994) postulated that flower development is sometimes significantly affected in some virus-host interactions, resulting in decreased seed set and consequently reduced potential for seed transmission. This is illustrated by the example of differential seed transmission of *Tobacco streak virus* (TSV) strains A and W. Ghanekar and Schwenk (1974) and Johansen *et al*. (1994) suggested that early infection by A-TSV results in seed transmission, whereas early inoculation of W-TSV reduces flower formation and therefore prevents seed development in host plants. The analyses presented by Yang and Hamilton (1974) have shown, that *Tobacco ringspot virus* (TRSV) inoculation of soybeans also results in necrotic changes in flowers and buds, developing an infections close to 100% incidence in host seeds. Our previous findings with *Tobacco rattle virus* (Tobravirus) revealed that flower production was reduced by 37% in tobacco, whereas it was reduced by 49% in *Yolo Wonder C. annuum* plants (Otulak *et al.,* 2016). Furthermore, our findings on PVY^{NTN} infection showed a decrease of 38.6% in the number of *Capsicum* flowers and fruits in comparison with healthy plants. Theoretically, reduced numbers of flowers and fruits reduced also the level of seed transmission, so we determined a 28% decline in the number of seeds compared to healthy *C. annuum* plants. Despite this, we noticed 30% seeds contained PVY^{NTN} particles, and consequently seed transmission of this potyvirus is still possible. Examination of these seeds also showed that most were also able to germinate. Between germinated F1 generation plants, a significant number were infected by PVY^{NTN} (about 30%). This indicates that PVY can be transmitted to seeds, and from them to next generation hosts with stable frequency.

There is no precise answer as to how plant viruses cross the barriers between the parent and progeny tissues in ovules in direct embryo cell infection, and there are no suggested routes by which the virions enter the elements of developing embryos, as postulated by Johansen *et al.* (1994) and Wang and Maule (1994). It is now clearly understood that there are two pathways to infection of developing embryos, either by indirect invasion through infection of the gametes before the fertilization process or by direct embryo invasion after fertilization. For many virus–host interactions, both modes of embryo infection may result in maximum seed transmission (Johansen *et al.,* 1994). The seed-transmitted viruses that invade directly after fertilization are found in different seed tissues, and may be confined to embryo or endosperm tissues. In such cases, the infections originate at female gamete production. Many examples of internally seed-transmitted viruses are known, including; *Pea seed-borne mosaic virus* (PSbMV), *Southern-Bean mosaic virus* (SBMV), and or *Lettuce mosaic virus* (LMV). These viruses have been internally detected in cotyledons and embryos of their respective hosts (Wang *et al.,* 1997; Yang *et al.,* 1997; de Assis and Sherwood, 2000; Roberts *et al.,* 2003; Ali and Kobayashi, 2010). Our ultrastructural study has demonstrated, for the first time, PVY^{NTN} particles and PVY cytoplasmic inclusions within cells of host ovarian walls, parenchyma cells and also in phloem and xylem elements. PVY^{NTN} particles and intense virus localization have

been detected in *Capsicum* placentae. PVY^{NTN} particles were observed in integument cells of the ovules and in nucelli. However, the embryo sacs have, so far, not been shown to contain virions.

Distribution of viruses within seeds was studied by bioassay/serology and electron microscopy. Some viruses, such as BSMV and TMV, infect the endosperm tissues (Carroll, 1972). Hoch and Provvidenti (1978) provided electron micrographic evidence for localization of *Bean common mosaic virus* (BCMV) particles and viral inclusion bodies in mature embryos of dormant and germinating bean seeds. They have also recorded virus in thin sections of embryo and endosperm tissues of infected soybean seeds (Tu, 1975; 1989). Our study has demonstrated PVY^{NTN} particles and virus cytoplasmic inclusions in *C. annuum* integument parenchyma cells and collapsed endothelial layers (between endosperm and integument), as well as on the embryos, which was confirmed by PVY immunolocalization. Our analysis of derived from infected plants demonstrated PVY^{NTN} virions in degenerated and altered integument parenchyma cells, as well as in endothelial layers, resulting from PVY virions in ovules. Embryo invasion by *Turnip yellow mosaic virus* (TYMV), another potyvirus, in *Arabidopsis thaliana*, was also reported by de Assis and Sherwood (2000). Some of the embryo-borne potyviruses identified include PSbMV in pea (Wang and Maule, 1994; Roberts *et al.,* 2003; Card *et al.*, 2007), BCMV in bean (Hoch and Provvidenti, 1978), and SMV in soybean (Bowers and Goodman, 1979). A previous study has shown that PSbMV infects host embryos directly through symplastic connections between the maternal cells and the embryos (Roberts *et al.,* 2003). From the maternal tissue, PSbMV enters the endosperm through plasmodesmata between the endosperm cells and seed testa. During early seed development stages, PSbMV invades the suspensor cells through transient vesicles, which are present at the base of the suspensor in the micropylar region where the suspensor is anchored to the endosperm. Further virus enters the embryos from the suspensor through plasmodesmata. However, at early seed development, the presence of the virus in the micropylar region is necessary for the seed transmission (Roberts *et al.*, 2003).

Electron microscopy analyses revealed BSMV (Caroll, 1974) and TRSV particles within infected pollen grains (Caroll, 1974; Yang and Hamilton, 1974). In investigations using RT-PCR, dot-blot, or *in situ* hybridization, it has been shown that *Prunus necrotic ringspot virus* particles (PNRSV) infect host pollen grains (Aparicio, 1999; Amari *et al.,* 2007). The BSMV virions were found in sperm cells and were distributed in tissues connected with embryogenesis (Brlansky *et al.,* 1986; Hull, 2002). Immunogold localization of *Alfalfa mosaic virus* (AMV) indicated particle distribution in anthers of alfalfa (Pesic *et al.,* 1988; Hull, 2002). Our investigation has demonstrated PVY^{NTN} particles and inclusions in residues of tapetum cells among osmophilic masses and necrotized anther cells. Dispersed viral particles were observed in differentiated endothecium cells. The analysis demonstrated PVY^{NTN} particles in the cell nuclei of *C. annuum* pollen grains and on the exine. PVY^{NTN} cytoplasmic inclusions were also noted inside the degenerated pollen grains in the osmophilic cytoplasm. Immunofluorescence analysis of infected *C. annuum* anthers demonstrated more intense signals than in the case of *Tobacco rattle virus* detection (Otulak *et al.,* 2016). In PVY^{NTN} infections, fluorescence signals especially revealed remnants of tapetum masses together with pollen grains. Deposition also occurred in pollen tubes, in a manner similar to that for PNRSV (Amari *et al.,* 2007). This localization of PVY^{NTN} virions in pollen may be the potential route for virion transfer to the female gametophytes through the protoplasts of the vegetative cells. Immunogold labelling of PVY epitopes revealed their deposition in the mature *C. annuum* anther chambers, but also inside pollen grains. Our observations were similar to those of Hunter and Bowyer (1994). They showed gold-labelled LMV particles on the exine of lettuce pollen grains in all tested plants, but, differing from our results, LMV virions were observed inside pollen grains from only one plant. The tapetum, epidermis and endothecium of mature anthers from lettuce contained many LMV virions as well as pinwheel inclusions (Hunter and Bowyer, 1994; 1997). *Prunus necrotic ringspot virus* invaded host anthers, firstly infecting the vascular tissues of stamens (Amari *et al.*, 2007). Amari and coauthors (2007) postulated that PNRSV is able to move from the vasculature to infect connective tissues, through plasmodesmata. Virions are transferred to the tapetum and then, the pollen mother cells (PMC). As these authors suggested, pollen mother cells are invaded before callose deposition takes place, because no connections have been described in the callose layers similar to those present in plasmodesmata,

which were able to separate pollen mother cells from other anther tissues. Our results indicated that as pollen grains and anthers mature, intensity of PVY^{NTN} detection increases, and this is not due only to virus distribution.

Conclusions

There have been no previously reported studies on the potential effects of PVY^{NTN} infection on the development of host plant generative flower organs, in particular female and male gametophytes. This is the first detailed report on the impacts of PVY^{NTN} infection on *C. annuum* generative organs, including anthers, ovaries, seeds and consequently also in progeny plants. We postulate that PVY virions could be present on the exine on the surfaces of pollen, and also inside *C. annuum* pollen grains, which may have significance in the self-pollinated plants. We also report the presence of the PVY epitope in pollen tubes, confirmed by immunodetection. This investigation has indicated that PVY^{NTN} particles can be detected inside *C. annuum* seeds on the surface of embryos, and viral particles and inclusions were observed in endothelial layers. Virus was not detected inside the female gametophytes, but, PVY particles and cytoplasmic inclusions were mainly detected inside the ovaries, in the ovule integument and nucelli, which was confirmed by immunodetection. Evidence from this study suggests that there are two possible sources of PVY^{NTN} infection during the double fertilization process: the more likely source is via pollen grains (and pollen tubes) as an infection source in seeds, and the second is virus transfer via the integuments from which the seed coat is derived. These findings have important implications for management of PVY diseases, which requires detailed understanding of the epidemiology of this important plant virus.

Acknowledgements

The authors thank Ewa Znojek for her excellent technical assistance.

Compliance with ethical standards

The authors declared that no competing interests exist.

Literature cited

Ali A. and M. Kobayashi, 2010. Seed transmission of cucumber mosaic virus in pepper. *Journal of Virological Methods* 163, 234–237.

Amari K., L. Burgos, V. Pallas and M.A. Sanchez-Pina, 2007. *Prunus necrotic ringspot virus* Early Invasion and Its Effects on Apricot Pollen Grain Performance. *Virology* 97, 892–899.

Aparicio F., M.A. Sanchez-Pina, J.A. Sanchez-Navarro and V. Pallas, 1999. Location of *Prunus necrotic ringspot ilarvirus* within pollen grains of infected nectarine trees: evidence from RT-PCR, dot-blot and in situ hybridisation. *European Journal of Plant Pathology* 105, 623–627.

Arroyo R., M.J. Soto, J.M. Martinez-Zapater and F. Ponz, 1996. Impared cell-to-cell movement of *Potato virus Y* in pepper plants carrying the y^a (pr2) resistance gene. *Molecular Plant Microbe Interactions* 9, 314–318.

Bashar T., 2015. Characterization of Seed Transmission of Soybean Mosaic Virus in Soybean. PhD Thesis, The University of Western Ontario, London, Canada, 14–16 pp.

Beczner L., J. Horvath, I. Romhanyi and H. Forster, 1984. Studies on the aetiology of tuber necrotic ringspot disease in potato. *Potato Research* 27, 339–352.

Blanchard A., M. Rolland, C. Lacroix, C. Kerlan and E. Jacquot, 2008. *Potato virus Y*: a century of evolution. *Current Topics in Virology* 7, 21–32.

Bowers G.R. Jr. and R.M. Goodman, 1979. Soybean mosaic virus: infection of soybean seed parts and seed transmission. *Phytopathology* 69, 569–572.

Brlansky R.H., T.W. Carroll and S.K. Zaske, 1986. Some ultrastructural aspects of the pollen transmission of barley stripe mosaic virus in barley. *Canadian Journal of Botany* 64, 853–858.

Cai X.K., D.M. Spooner and S.H. Jansky, 2011. A test of taxonomic and biogeographic predictivity: Resistance to potato virus Y in wild relatives of the cultivated potato. *Phytopathology* 101, 1074–1080.

Card S.D., M.N. Pearson and G.R.G. Clover, 2007. Plant pathogens transmitted by pollen. *Australasian Plant Pathology* 36(5), 455–461.

Carroll T.W., 1972. Seed transmissibility of two trains of barley stripe mosaic virus. *Virology* 48, 323–336.

Carroll T.W., 1974. Barley stripe mosaic virus in sperm and vegetative cell of barley pollen. *Virology* 60, 121–128.

Carroll T.W., 1981. Seedborne viruses: virus–host interactions. In: *Plant Diseases and Vectors: Ecology and Epidemiology* (K.F. Harris, ed.), Academic Press, New York, USA, 293–317.

Chrzanowska M. and T. Doroszewska, 1997. Comparison between PVY isolates obtained from potato and tobacco plants grown in Poland. *Phytopathologica Polonica* 8, 15–20.

de Assis F.M. and J.L. Sherwood, 2000. Evaluation of seed transmission of *Turnip yellow mosaic virus* and *Tobacco mosaic virus* in *Arabidopsis thaliana*. *Phytopathology* 90, 1233–1238.

Draper M.D., J.S. Pasche and N.C. Gudmestad, 2002. Factors influencing PVY development and disease expression in three potato cultivars. *American Journal of Potato Research* 79, 155–165.

Fink H., 1960. Epoxy resins in electron microscopy. *Journal of Biophysical and Biochemical Cytology* 7(1), 27–30.

Ghanekar A.M. and F.W. Schwenk, 1974. Seed transmission and distribution of tobacco streak virus in six cultivars of soybeans. *Phytopathology* 64, 112–114.

Gubler F., 1989. Immunofluorescence localization of microtubules in plant root tip embedded in buthyl-methyl-methacrylate. *Cell Biology International Reports* 13, 137–145.

Hoch H.C. and R. Provvidenti, 1978. Ultrastructural location of bean common mosaic virus in dormant and germinating seeds of *Phaseolus vulgaris*. *Phytopathology* 68, 327–330.

Hull R., 2002. *Matthew's Plant Virology*. Academic Press, New York, NY, USA.

Hull R., 2004. Transmission 2: mechanical, seed, pollen and epidemiology. In: *Matthews' plant virology* (R. Hull, ed.), Elsevier Academic Press, The Netherlands, 533–582.

Hunter D.G. and J.W. Bowyer, 1994. Cytopathology of Anthers and Pollen From Lettuce Plants Infected by *Lettuce Mosaic Virus*. *Journal of Phytopathology* 142, 107–114.

Hunter D.G. and J.W. Bowyer, 1997. Cytopathology of developing anthers and pollen mother cells from lettuce plants infected by Lettuce mosaic potyvirus. *Journal of Phytopathology* 145, 521–524.

Johansen E., M.C. Edwards and R.O. Hampton,1994. Seed transmission of viruses: current perspectives. *Annual Review of Phytopathology* 32, 363–386.

Johnson A.A., T. Vidya, S. Papaiah, M. Srinivasulu, B. Mandal and D.S. Gopal, 2013. First Report of *Zucchini yellow mosaic virus* Infecting Gherkin (*Cucumis anguira*) in India. *Indian Journal of Virology* 24, 289–290.

Karnovsky M.J., 1965. A formaldehyde – glutaraldehyde fixative of high osmolarity for use in electron microscopy. *Journal of Cell Biology* 27, 137–138.

Kerlan C., 2006. Potato virus Y. Descriptions of Plant Viruses no. 414. *Association of Applied Biologists*. http://www.dpvweb.net/dpv/showdpv.php?dpvno=414. Accessed 3 November 2016.

Khan M.S., M.I. Hoque, R.H. Sarker and H.P. Muehlbach, 2003. Detection of important plant viruses in *in vitro* regenerated potato plants by Double Antibody Sandwich Method of ELISA. *Plant Tissue Culture* 13(1), 21–29.

Mayhew T. M., 2011. Quantifying immunogold localization on electron microscopic thin sections: a compendium of new approaches for plant cell biologists. *Journal of Experimental Botany* 62(12), 4101–4113.

Nováková S., G. Flores-Ramírez, M. Glasa, M. Danchenko, R. Fiala and L. Skultety, 2015. Partially resistant Cucurbita pepo showed late on set of the *Zucchini yellow mosaic virus* infection due to rapid activation of defense mechanisms as compared to susceptible cultivar. *Frontiers in Plant Science* 6(263), 1–14.

Otulak K. and G. Garbaczewska, 2010. Ultrastructural events during hypersensitive response of potato cv. Rywal infected with necrotic strains of potato virus Y. *Acta Physiologiae Plantarum* 32, 635–644.

Otulak K. and G. Garbaczewska, 2012. Cytopathological *Potato virus Y* structures during *Solanaceous* plants infection. *Micron* 43, 839–850.

Otulak K. and G. Garbaczewska, 2014. The participation of plant cell organelles in compatible and incompatible potato virus Y-tobacco and -potato plant interaction. *Acta Physiologiae Plantarum* 36, 85–99.

Otulak K., E. Kozieł and G. Garbaczewska, 2016. Ultrastructural impact of *Tobacco Rattle Virus* on tobacco and pepper ovary and anther tissues. *Journal of Phytopathology* 164, 226–241.

Palloix A., V. Ayme and B. Moury, 2009. Durability of plant major resistance genes to pathogens depends on the genetic background, experimental evidence and consequences for breeding strategies. *New Phytologist* 183, 190–199.

Pesic Z., C. Hiruki and M.H. Chen, 1988. Detection of viral antigen by immunogold cytochemistry in ovules, pollen, and anthers of alfalfa infected with alfalfa mosaic virus. *Phytopathology* 78, 1027–1032.

Quenouille J., N. Vassilakos and B. Moury, 2013. Potato virus Y: a major crop pathogen that has provided major insights into the evolution of viral pathogenicity. *Molecular Plant Pathology* 14, 439–452.

Roberts I. M., D. Wang, C.L. Thomas and A.J. Maule, 2003. Pea seed-borne mosaic virus seed transmission exploits novel symplastic pathways to infect the pea embryo and is, in part, dependent upon chance. *Protoplasma* 222, 31–43.

Simmons H.E., J.P. Dunham, K.E. Zinn, G.P. Munkvold, E.C. Holmes and A.G. Stephenson, 2013. Zucchini yellow mosaic virus (ZYMV, Potyvirus): vertical transmission, seed infection and cryptic infections. *Virus Research* 176, 259–264.

Stace-Smith R. and R.I. Hamilton, 1988. Inoculum thresh holds of seedborne pathogens: viruses. *Phytopathology* 78, 875–880.

Tu J.C., 1975. Localization of infections soybean mosaic virus in mottled soybean seeds. *Microbiology* 14, 151–156.

Tu J.C., 1989. Effect of different strains of soybean mosaic virus on growth, maturity, yield, seed mottling and seed transmission in several soybean cultivars. *Journal of Phytopathology* 126, 231–236.

Van Lent J.W. and B.J.M. Verduin, 1986. Detection of viral protein and particles in thin sections of infected plant tissue using immunogold labelling. In: *Developments in Applied Biology I. Developments and Applications in Virus Testing* (R.A.C. Jones, L. Torrance, ed.), Association of Applied Biologists Wellesbourne, UK, 193–211.

Wang D., S.A. MacFarlane and A.J. Maule, 1997. Viral determinants of pea early browning tobravirus seed transmission in pea. *Virology* 234, 112–117.

Wang D. and A.J. Maule, 1994. A model for seed transmission of a plant virus: Genetic and structural analyses of Pea embryo invasion by Pea seed-borne mosaic virus. *The Plant Cell* 6, 777–787.

Yang A.F. and R.I. Hamilton, 1974. The mechanism of seed transmission of tobacco ringspot virus in soybean. *Virology* 62, 26–37.

Yang Y., K.S. Kim and E.J. Anderson, 1997. Seed transmission of cucumber mosaic virus in spinach. *Phytopathology* 87, 924–931.

Accepted for publication: September 19, 2017